Accompanying material – The “teapot in a city”: a paradigm shift in urban climate modeling

Najda Villefranque,[1*] Frédéric Hourdin,[1] Louis d’Alençon,[1]
Stéphane Blanco,[2] Olivier Boucher,[1] Cyril Caliot,[3]
Christophe Coustet,[4] Jérémi Dauchet,[5] Mouna El Hafi,[6]
Vincent Eymet,[4] Olivier Farges,[7] Vincent Forest,[4]
Richard Fournier,[2] Jacques Gautrais,[8] Valéry Masson,[9]
Benjamin Piaud,[4] Robert Schoetter,[9]

[1]LMD/IPSL/SU, CNRS, Paris, 75005, France,
[2]Laplace, INP/Université de Toulouse/CNRS, Toulouse, France,
[3]LMAP, CNRS, UPPA, E25, Anglet, France,
[4]Méso-Star, Longages, France,
[5]Institut Pascal, Université Clermont Auvergne, Clermont Auvergne INP, CNRS, Clermont-Ferrand, France,
[6]Centre RAPSODEE, Université de Toulouse, Mines Albi, UMR CNRS 5302, Campus Jarlard, Albi, France,
[7]LEMTA, Université de Lorraine, CNRS, Nancy, France,
[8]CRCA, CBI, Université de Toulouse, CNRS, Toulouse, France,
[9]CNRM, Université de Toulouse, Météo-France, CNRS, Toulouse, France

[*]To whom correspondence should be addressed; E-mail: najda.villefranque@lmd.ipsl.fr

March 2, 2022

This document consists of two sections describing the models used to produce Figure 2 and Figure 4 of the main manuscript.

1 A simple example of a path-integral reformulation of physics

This section presents the full developments associated with the “simple example of a path-integral reformulation of physics” which was only briefly described in the main document.

1.1 The one-room building

In relation with Fig. 3a

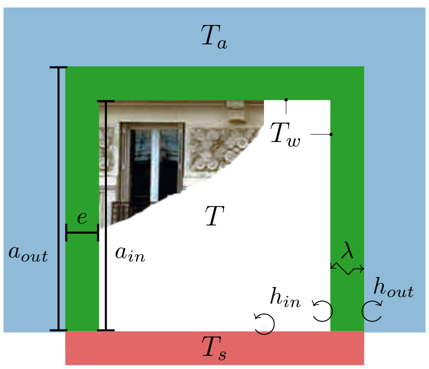

Inside wall convective thermal conductance: $H_{in} = h_{in} a_{in}$

Outside wall convective thermal conductance: $H_{out} = h_{out} a_{out}$

Wall thermal conductance: $C_w = a_{in} \lambda / e$

Wall+outside overall thermal conductance: $U_w = \dfrac{C_w \times H_{out}}{C_w + H_{out}}$

Figure S1. Illustration of the one-room building.

Let us consider the 2D one-room building that is illustrated in Fig. S1. The objective is to estimate T, the temperature of the perfectly-mixed air inside the room. The heat flux at the inner face of any of the four walls is modeled as:

$$Q = h_{in} a_{in} \Delta T \tag{1}$$

where h_{in} is a lineic convective heat transfer coefficient in $\mathrm{Wm^{-1}K^{-1}}$, assumed to be the same for the four walls, a_{in} is the length of the segment wall in m, assumed to be the same for the four walls (square room) and ΔT is the difference between the temperature near the wall and the temperature of the wall. $H_{in} = h_{in} a_{in}$ is the convective thermal conductance associated with any of the interior walls, in $\mathrm{WK^{-1}}$. The temperature of the lower wall, i.e. the ground floor, is T_s, and the inner temperature of the three other walls is T_w, which is assumed to be the same everywhere (the ground floor is isolated from the walls).

The steady-state energy balance inside the room is:

$$\underbrace{H_{in}(T_s - T)}_{\text{ground floor}} + \underbrace{H_{in}(T_w - T)}_{\text{left wall}} + \underbrace{H_{in}(T_w - T)}_{\text{right wall}} + \underbrace{H_{in}(T_w - T)}_{\text{ceiling}} = 0 \tag{2}$$

from which we deduce:

$$T = \frac{H_{in}}{H_{in} + 3H_{in}} T_s + \frac{3H_{in}}{H_{in} + 3H_{in}} T_w = \frac{1}{4} T_s + \frac{3}{4} T_w \tag{3}$$

In relation with Fig. 3b If T_w is known, then T can be estimated using the following Monte Carlo algorithm:

1. Repeat N times:
   (a) Sample u uniformly inside $[0, 1]$
   (b) If $u < 1/4$: $T_i = T_s$
   (c) else: $T_i = T_w$
2. Compute the average T_i over the N realizations

The simulated random experiment is equivalent to tossing an unbalanced coin and retaining different temperatures for head and tail outcomes.

In relation with Fig. 3c We now assume that T_w is unknown. The steady-state energy balance of a wall of temperature T_w is:

$$\underbrace{U_w(T_a - T_w)}_{\text{outside transfer}} + \underbrace{H_{in}(T - T_w)}_{\text{room transfer}} = 0 \tag{4}$$

where U_w is the overall thermal conductance, which models the combined effect of conduction through the wall and convective exchange with the environmental air. We deduce:

$$T_w = \frac{U_w}{U_w + H_{in}} T_a + \frac{H_{in}}{U_w + H_{in}} T = p_a T_a + (1 - p_a) T \tag{5}$$

with $p_a = \frac{U_w}{U_w + H_{in}}$.

Coupling Equation (3) and Equation (5) yields a recursive equation for T:

$$T = p_s T_s + (1 - p_s) \left[p_a T_a + (1 - p_a) T \right] \tag{6}$$

with $p_s = \frac{1}{4}$. In this very simple example, the expression can be factorized:

$$\begin{aligned} T &= p_s T_s + (1 - p_s) p_a T_a + (1 - p_s)(1 - p_a) T \\ &= (p_s T_s + (1 - p_s) p_a T_a) \sum_{n=0}^{\infty} ((1 - p_s)(1 - p_a))^n \\ &= (p_s T_s + p_b T_a) \sum_{n=0}^{\infty} (1 - p_s - p_b))^n \end{aligned} \tag{7}$$

with $p_b = p_a(1 - p_s)$. Since $\sum_{n=0}^{\infty} r^n = 1/(1 - r)$,

$$T = \frac{p_s}{p_s + p_b} T_s + \frac{p_b}{p_s + p_b} T_a \tag{8}$$

Note that this result can also be obtained using the overall thermal conductance of the whole inside+wall+outside system, $U = \frac{H_{in} U_w}{U_w + H_{in}}$, and writing the steady-state energy balance $H_{in}(T_s - T) + 3\,U(T_a - T) = 0$ and hence $\frac{p_s}{p_s + p_b} = \frac{H_{in}}{H_{in} + 3U}$.

Equation (8) resembles Equation (3) and T can be estimated using a similar algorithm with the appropriate probability set and associated outcomes:

1. Repeat N times:
   (a) Sample u uniformly inside $[0, 1]$
   (b) If $u < \frac{p_s}{p_s + p_b}$: $T_i = T_s$
   (c) else: $T_i = T_a$
2. Compute the average T_i over the N realizations

Real-world problems are rarely that simple and most often, a closed-form expression cannot be written and sampled analytically. Instead, the complex global problem is cut into simpler, local problems. Going back to the recursive expression of Equation (6), the following algorithm can be used to estimate T *without deriving the closed-form expression*, thanks to double randomization:

1. Repeat N times:

   Repeat until an outcome is found:
   (a) Sample u uniformly inside $[0, 1]$
   (b) If $u < p_s$: $T_i = T_s$
   (c) else:
      i. Sample v uniformly inside $[0, 1]$
      ii. If $v < p_a$: $T_i = T_a$
      iii. else: no outcome has been found yet ; go to (a)
2. Compute the average T_i over the N realizations

1.2 The N×M rooms building

In this second example, the one-room model is extended to simulate heat propagation in a building made of N stories and M rooms per floor. The external boundary conditions are the same as in the one-room model, that is, the temperature T_a of the perfectly-mixed outside air and the temperature T_s of the ground floor of the building are known, and the boundary walls are characterized by their overall (conducto-convective) thermal coefficient U_w. The one room is divided into $N \times M$ rooms separated by thin walls; heat conduction is neglected in these interior walls. The rooms are square and the convective thermal conductance H_{in} is constant throughout the building. The objective is to compute $T_{i,j}$, the temperature of the perflectly-mixed air in the j^{th} room on the i^{th} floor.

The steady-state energy balance of a room is, for all $1 \leq i \leq N$ and $1 \leq j \leq M$:

$$\underbrace{H_{in}(T_{i-\frac{1}{2},j} - T)}_{\text{bottom wall}} + \underbrace{H_{in}(T_{i+\frac{1}{2},j} - T)}_{\text{top wall}} + \underbrace{H_{in}(T_{i,j-\frac{1}{2}} - T)}_{\text{left wall}} + \underbrace{H_{in}(T_{i,j+\frac{1}{2}} - T)}_{\text{right wall}} = 0 \tag{9}$$

hence

$$T_{i,j} = \frac{1}{4}T_{i-\frac{1}{2},j} + \frac{1}{4}T_{i+\frac{1}{2},j} + \frac{1}{4}T_{i,j-\frac{1}{2}} + \frac{1}{4}T_{i,j+\frac{1}{2}} \tag{10}$$

where $T_{i-\frac{1}{2},j}$, $T_{i+\frac{1}{2},j}$, $T_{i,j-\frac{1}{2}}$ and $T_{i,j+\frac{1}{2}}$ are respectively the inner temperatures of the bottom, top, left and right walls of room (i,j). The first step of the Monte Carlo algorithm to compute $T_{i,j}$ is thus to sample one of the room walls, each with probability $\frac{1}{4}$. In case the temperature of the sampled wall is unknown, the steady-state energy balance on the interface wall gives, for example for the wall $(i-\frac{1}{2},j)$ between room (i,j) and room $(i-1,j)$:

$$H_{in}(T_{i-\frac{1}{2},j} - T_{i-1,j}) + H_{in}(T_{i-\frac{1}{2},j} - T_{i,j}) = 0 \tag{11}$$

and hence

$$T_{i-\frac{1}{2},j} = \frac{1}{2}T_{i-1,j} + \frac{1}{2}T_{i,j} \tag{12}$$

which generalizes to:

$$\begin{aligned} T_{i\pm\frac{1}{2},j} &= p_{i\pm\frac{1}{2},j}T_{i\pm1,j} + (1 - p_{i\pm\frac{1}{2},j})T_{i,j} \\ T_{i,j\pm\frac{1}{2}} &= p_{i,j\pm\frac{1}{2}}T_{i,j\pm1} + (1 - p_{i,j\pm\frac{1}{2}})T_{i,j} \end{aligned} \tag{13}$$

with, for interior rooms (that are not adjacent to an exterior wall and not at ground floor):

$$\forall\, 1 < i < N \quad, \forall\, 1 < j < M, \quad p_{i-\frac{1}{2},j} = p_{i+\frac{1}{2},j} = p_{i,j-\frac{1}{2}} = p_{i,j+\frac{1}{2}} = \frac{1}{2} \tag{14}$$

and for boundary rooms (adjacent to an exterior wall or at ground floor):

$$\begin{array}{llrlrl} \text{Ground floor surface:} & \forall 1 \leq j \leq M, & p_{\frac{1}{2},j} & = 1, & T_{0,j} & = T_s \\ \text{Upper floor ceiling:} & \forall 1 \leq j \leq M, & p_{N+\frac{1}{2},j} & = p_a, & T_{N+1,j} & = T_a \\ \text{Left hand wall:} & \forall 1 \leq i \leq N, & p_{i,\frac{1}{2}} & = p_a, & T_{i,0} & = T_a \\ \text{Right hand wall:} & \forall 1 \leq i \leq N, & p_{i,M+\frac{1}{2}} & = p_a, & T_{i,M+1} & = T_a \end{array} \tag{15}$$

with $p_a = \frac{U_w}{U_w+H_{in}}$ as in Equation (5). Note that with the chosen notations, $p_{i-\frac{1}{2},j}$ is the same on both sides of the wall. In the configuration described here, the interior walls are symmetric (the convective thermal conductance is the same on both sides), and the exterior walls can only be crossed in one direction (from inside to outside), so the notation is not ambiguous. However, a more general notation as for instance $p_{i\to i-1,j}$, would be necessary in cases where $p_{i-1\to i,j}$ (crossing the wall between $(i-1,j)$ and (i,j) from left to right) and $p_{i\to i-1,j}$ (crossing the same wall from right to left) are not necessary equal.

Coupling Equation (10) and Equation (13) yields:

$$\begin{aligned} T_{i,j} =& \frac{1}{4}(p_{i-\frac{1}{2},j}T_{i-1,j} + (1-p_{i-\frac{1}{2},j})T_{i,j}) + \frac{1}{4}(p_{i+\frac{1}{2},j}T_{i+1,j} + (1-p_{i+\frac{1}{2},j})T_{i_j}) \\ &+ \frac{1}{4}(p_{i,j-\frac{1}{2}}T_{i,j-1} + (1-p_{i,j-\frac{1}{2}})T_{i,j}) + \frac{1}{4}(p_{i,j+\frac{1}{2}}T_{i,j+1} + (1-p_{i,j+\frac{1}{2}})T_{i,j}) \end{aligned} \tag{16}$$

Relying on double randomization, Equation (16) is sampled recursively until reaching one of the boundary rooms, in which either a boundary condition is sampled thereby ending the realization (or *path*), or a neighboring room is sampled in which case the path continues. The example illustrated in Fig. 3**f** of the main manuscript includes a "thermal bridge". The convective thermal conductance in the rooms inside the thermal bridge region were set to larger values than elsewhere in the building. From an adjacent room, the probability of entering the thermal bridge region is therefore much higher than the probability of moving to any of the three other neighboring rooms. Once in the thermal bridge, the probability of exiting is much smaller than that of remaining inside. The conductive heat transfer coefficient of the outer wall in the thermal bridge region has been set to higher value than in the rest of the exterior walls, which is symptomatic of bad thermal isolation.

Fig. S2 shows the computing time per path (a), and the steady-state temperature in the target room (b), for each of the cases shown in Fig. 3d,e,f of the main manuscript ($T_s = 30^\circ$ C, $T_a = 10^\circ$ C), and as a function of the number of stories (in the main manuscript, the simulations are made with N=32). Each estimate is the average of 10k realizations. The target room in Fig. 3e is closer to the boundary wall than that of Fig. 3d, resulting in colder temperatures. Including a thermal bridge leads to colder temperatures and increases the computing time because paths are trapped hence more steps are necessary on average to find an outcome. As the number of storeys increases, the target rooms become relatively further from the top floor boundary, resulting in longer paths (longer computation time). Once the top floor is more than 20 stories above the target room, temperature and the computing times become insensitive to the number of stories. This feature is specific to the "probe" Monte Carlo approach, in which paths start at the sensor location and randomly visit the system by sampling events on the basis of physical processes: the temperature of a

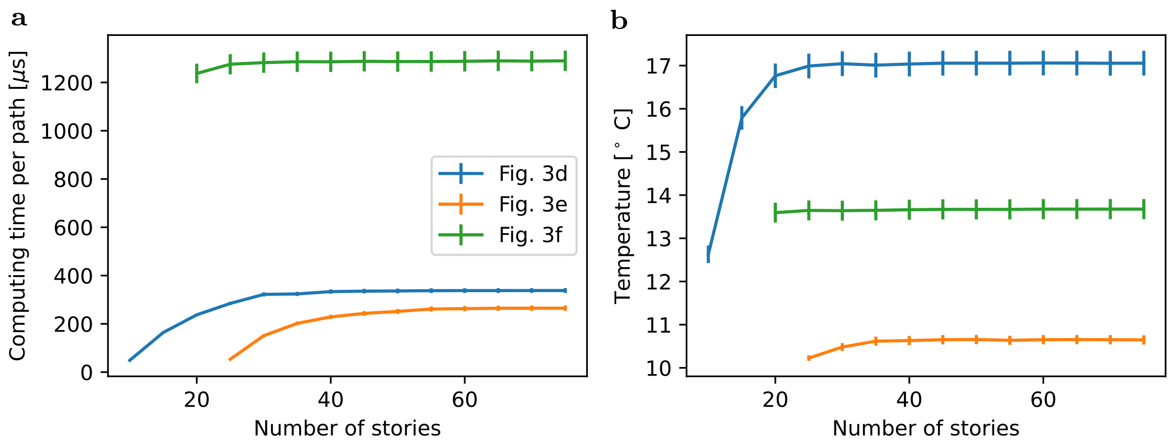

Figure S2. **a** Computing time per path, **b**, temperature in room (i,j), as functions of the number of stories in the building. Fig 3d: target room (10,8); Fig 3e: target room (25,22); Fig 3f: target room (10, 8) and thermal bridge. The error bars give the 99.7% confidence interval (10k paths per estimate).

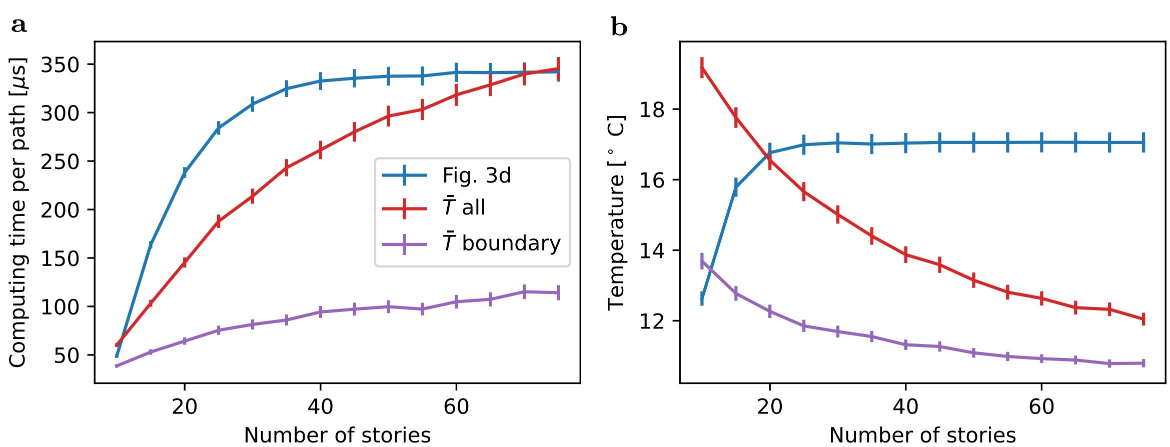

Figure S3. **a** Computing time per path, **b**, temperature, as functions of the number of stories in the building. Fig 3d: target room (10,8); $\bar{T}$ all: average over all the rooms; $\bar{T}$ border: average over the rooms that are adjactent to the exterior walls. The error bars give the 99.7% confidence interval (10k paths per estimate).

room in the lowest floors does not depend much on the conditions set in the far high floors, and few paths will visit these higher parts of the building.

With this probe approach, computing the average temperature over multiple rooms does not necessarily increase the computing time with respect to the time associated with a randomly-chosen single-room estimate. Fig S3 shows that the computing time associated with temperatures averaged over all the building rooms or over the boundary rooms only can even be less than the computing time associated with the punctual estimate of Fig. 3d (room (10,8)).

The building heat loss can be estimated from the temperature averaged over the rooms that are adjacent to exterior walls $\bar{T}$, and the overall thermal conductance $U = \frac{H_{in} U_w}{H_{in} + U_w}$

$$\bar{Q} = U(\bar{T} - T_a) \tag{17}$$

where $\bar{Q}$ is the average heat loss per boundary room and the net heat loss is simply the number of boundary rooms times $\bar{Q}$. Average lineic heat loss estimates ($\bar{Q}/a$) are shown in Fig. S4b for two experiments, one with $C_w = 1.2$ (paths shown in Fig. S4c), and one with $C_w = 12.$ (poor isolation, paths shown in Fig. S4d). Instead of sampling 10k paths, the simulation stops when the accuracy of the $\bar{Q}$ estimate reaches 0.01 W/m. The total simulation time is displayed in Fig. S3a. In the first experiment, individual paths are longer but the required accuracy is reached with fewer paths, hence the total computing time is shorter. The lineic heat loss amplitude decreases when the number of stories increases because the density of outer rooms (and hence of the exposed surface) with respect to total number of rooms decreases.

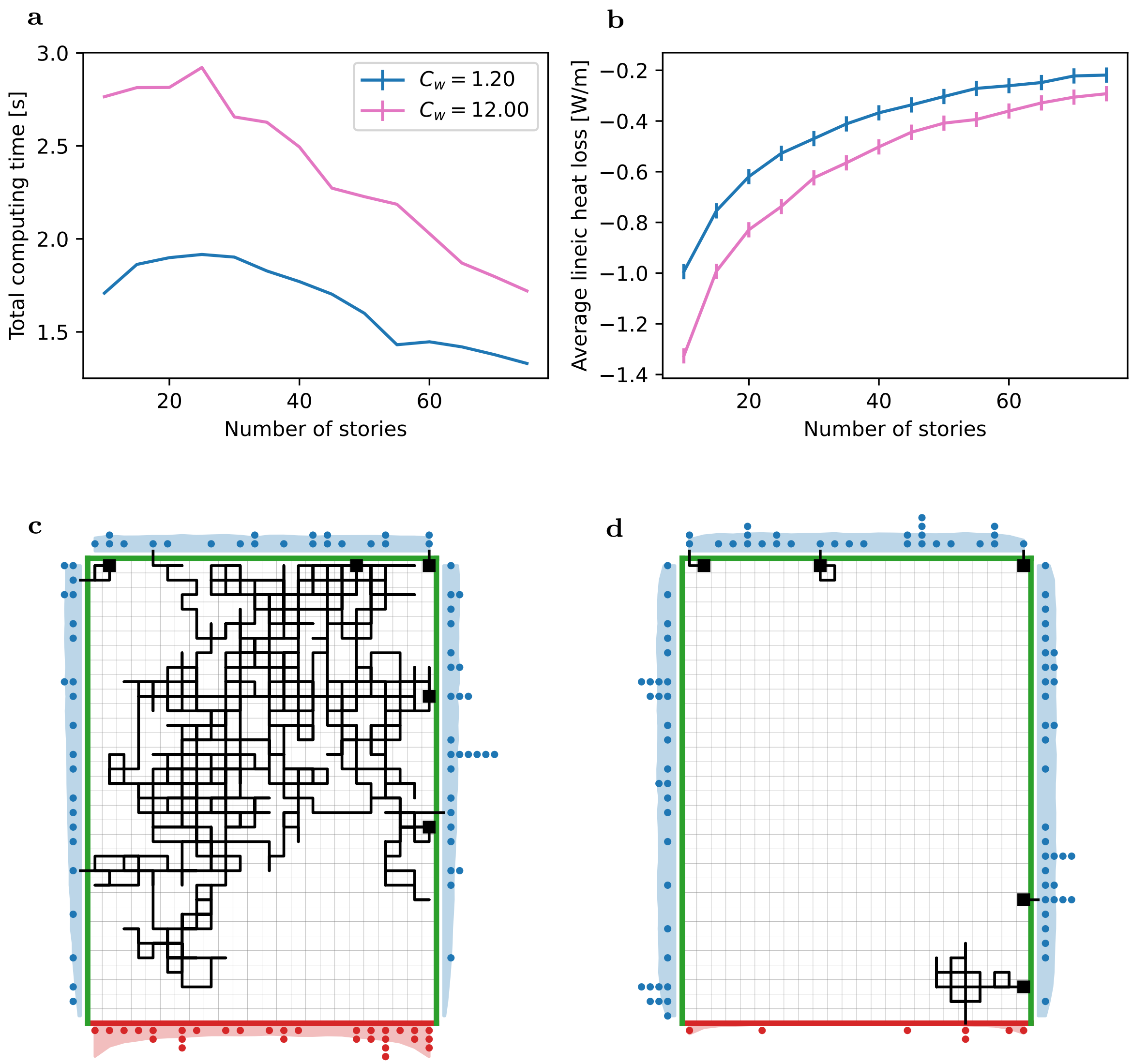

Figure S4. **a** Total computing time, **b**, average lineic heat loss, as functions of the number of stories in the building. $C_w = a\lambda/e$ is the wall conductance. The simuation stops when the standard deviation associated with the estimate reaches 0.01 W/m. The error bars give the 99.7% confidence interval (± 0.03 W/m). **c,d**, as Fig. 3d of the main manuscript but for the two experiments of **a,b**. Five paths are shown (black lines) and the boundary rooms are sampled at the beginning of each path (black squares).

2 Conduction in a solid interfaced with climate model outputs

2.1 The model formulation

The example in Fig. 5b,d of the paper was aimed at illustrating the ability of a Monte Carlo calculation to compute a quantity, the surface temperature T_s of soil, for which we have an estimation to compare with: the surface temperature of the meteorological archive. The soil model consists of a 8m-deep slab of solid material of volumic heat capacity $\rho_s Cp_s = 2.25$ MJ/(m^{3}K) and conductivity $\lambda = 1$ W/(mK). The values, typical of soil materials, were tuned in order to get a thermal inertia or effusivity $I_s = \sqrt{\rho_s Cp_s \lambda}$=1500 J m^{-2} K^{-1} s$^{-1/2}$. For an homogeneous soil, the thermal inertia is the unique characteristic of the soil material which enters into account in the behavior of the soil model and of its coupling with the atmosphere. The specific value was chosen after some tests to get a good representation of the amplitude of the diurnal cycle (see Fig. 5d).

The time evolution of the temperature T inside the solid, under the effect of conduction, reads as the divergence of the conductive flux:

$$\rho_c C_c \frac{\partial T_c}{\partial t} = -\vec{\nabla}.\left(-\lambda \vec{\nabla}\, T_c\right) \tag{18}$$

The coupling with the atmosphere is handled by the flux continuity equation:

$$F_{cond} = \mathbf{F_{SW}} + F_{LW} + F_{cv} - \mathbf{LE} \tag{19}$$

The notation $\mathbf{X}$ means here that the variable X is imposed, either read in the meteorological archive or directly derived from archived values. The first example consists in computing a surface temperature T_s and comparing it with the archived surface temperature $\mathbf{T_s}$.

The fluxes (oriented downward) that enter this equation are:

• F_{cond}, *the conduction flux below the surface*

$$F_{cond} = -\lambda \frac{\partial T}{\partial z} \tag{20}$$

where z is the depth computed positively downward from the surface.

• $\mathbf{F_{SW}}$, *the net solar flux* (SW standing for short-wave), imposed as $\mathbf{F_{SW}} = \mathbf{F^{\downarrow}_{SW}} - \mathbf{F^{\uparrow}_{SW}}$, both read from the meteorological archive.

• F_{LW}, *the net infra-red thermal flux* (LW for long-wave), computed as the difference between the (imposed) downward flux $\mathbf{F^{\downarrow}_{LW}}$ and the emission by the surface σT_s^4 where σ is the Stefan-Boltzmann constant and T_s the surface temperature, to be computed. In the simple version used here, the net flux is linearized as $F_{LW} = \mathbf{h_{rad}}(\mathbf{T_{rad}} - T_s)$ with $\mathbf{h_{rad}} = 4\sigma[(\mathbf{T_{rad}} + \mathbf{T_s})/2]^3$ where $\mathbf{T_{rad}}$ is the brightness temperature associated with the downward radiation, defined by $\mathbf{F}^{\downarrow}_{\mathbf{LW}} = \sigma \mathbf{T_{rad}}^4$. A non linear version has also been derived but the differences of the temperature in the linear and non linear algorithm are neglectable and the linear algorithm is privileged here for the sake of simplicity.

• F_{cv}*, the convective flux* (called turbulent or sensible heat flux in the climate science community) is compted as $F_{cv} = \mathbf{h_{cv}}(\mathbf{T_a} - T_s)$, where $\mathbf{T_a}$ is the archived 2-m air temperature (work is ongoing to include some coupling within the atmosphere with the installation so that $\mathbf{T_a}$ could be affected by the surface, as is the case for a UHI). The convective coefficient is computed from the (positive upward) archived sensible heat flux $\mathbf{H}$ and surface temperature $\mathbf{T_s}$, as $\mathbf{h_{cv}} = \mathbf{H}/(\mathbf{T_s} - \mathbf{T_a})$, keeping the value in the range $[0.2, 50]$ in m^2 s^{-1}.

• $-\mathbf{LE}$*, the latent heat flux* is imposed, L being the water latent heat of vaporization and E the surface evaporation (a flux of water in kg m$^{-}2$ s$^{-}1$).

The variables read in the archive are $\mathbf{F}^{\downarrow}_{\mathbf{SW}}$, $\mathbf{F}^{\uparrow}_{\mathbf{SW}}$, $\mathbf{F}^{\downarrow}_{\mathbf{LW}}$, $\mathbf{T_a}$, $\mathbf{T_s}$, $\mathbf{H}$ and $\mathbf{LE}$. The variables used to force the soil model are $\mathbf{F_{SW}}$, $\mathbf{T_{rad}}$, $\mathbf{h_{rad}}$, $\mathbf{T_a}$, $\mathbf{h_{cv}}$ and $\mathbf{LE}$.

2.2 Monte Carlo integration of the flux continuity equation

In order to integrate numerically the surface continuity equation, the conduction flux below the surface is discretized so that the surface flux continuity equation finally reads:

$$-\lambda \frac{T_d - T_s}{d} = \mathbf{h_{cv}}\left(\mathbf{T_a} - T_s\right) + \mathbf{h_{rad}}\left(\mathbf{T_{rad}} - T_s\right) + \mathbf{F_{SW}} - \mathbf{LE} \tag{21}$$

where T_d is the soil temperature at a small distance d below the surface. The equation is transformed to express T_s as the wheighted average of 3 temperatures:

$$T_s = \mathbf{p_{cv}}(\mathbf{T_a} + \xi) + \mathbf{p_{rad}}(\mathbf{T_{rad}} + \xi) + p_{cond}(T_d + \xi) \tag{22}$$

with

$$\begin{aligned} \Delta &= \mathbf{h_{cv}} + \mathbf{h_{rad}} + \lambda/d && (23)\\ \mathbf{p_{cv}} &= \mathbf{h_{cv}}/\Delta && (24)\\ \mathbf{p_{rad}} &= \mathbf{h_{rad}}/\Delta && (25)\\ p_{cond} &= \lambda/(d\Delta) && (26)\\ \xi &= \left(\mathbf{F_{SW}} - \mathbf{LE}\right)/\Delta && (27) \end{aligned}$$

The Monte Carlo formulation consists of shedding a probabilistic view on this average. With Probabilities $\mathbf{p_{cv}}$, $\mathbf{p_{rad}}$ and p_{cond} ($\mathbf{p_{cv}} + \mathbf{p_{rad}} + p_{cond} = 1$) the surface temperature takes values $\mathbf{T_a} + \xi$, $\mathbf{T_{rad}} + \xi$ or $T_d + \xi$ respectively. In the first two cases the temperature is given as a boundary condition of the problem (coming from the meteorological archive), the temperature is known and the path stops. In the third one, T_d is unknown. It will itself be considered as the average of a stochastic process for which only one realization is sampled, thus initiating a random walk in the soil as explained below.

2.3 δ-sphere computation of the conduction in the solid

The conduction equation inside the ground is approximated numerically by integrating it on a small sphere of radius r of volume Ω_r and surface Σ_r centered at point $\vec{x}$:

$$\int_{\Omega_r} \rho_s C p_s \frac{\partial T(\vec{x'}, t)}{\partial t} d\vec{x'} = \int_{\Omega_r} \lambda \vec{\nabla}.\vec{\nabla} T(\vec{x'}, t) d\vec{x'} \tag{28}$$

$$= \int_{\Sigma_r} \lambda \vec{\nabla} T(\vec{y'}, t).\vec{n}(\vec{y'}) d\vec{y'} \tag{29}$$

$$\simeq \int_{\Sigma_r} \frac{\lambda}{2r} \left[T(\vec{x} + 2r\ \vec{n}(\vec{y'}), t) - T(\vec{x}, t) \right] d\vec{y'} \tag{30}$$

Equation 28 is first transformed with the Green-Ostrogradski theorem (29) ($\vec{n}(\vec{y'})$ being the outward normal vector to the r-sphere) at $\vec{y'}$, and then approximated by a second order approximation of the gradient term (30). By considering the δ-sphere of radius $\delta = 2r$ (of volume $\Omega_\delta = 8\Omega_r$ and surface $\Sigma_\delta = 4\Sigma_r$), and replacing volumetric or surfacic integrals of $T(\vec{x'}, t)$ by the central value of $T(\vec{x}, t)$ times the volume or surface of integration (a second order estimate as well), it comes

$$\rho_s C p_s \frac{\Omega_\delta}{8} \frac{\partial T(\vec{x}, t)}{\partial t} = \frac{\Sigma_\delta}{4} \frac{\lambda}{\delta} (\overline{T}^\delta(\vec{x}, t) - T(\vec{x}, t)) \tag{31}$$

where $\overline{T}^\delta(\vec{x}, t)$ is the averaged temperature at time t over of the δ-sphere centered in x, $\overline{T}^\delta(\vec{x}, t) = \frac{1}{\Sigma_\delta} \int_{\Sigma_\delta} T(\vec{x}, t') d\vec{x'}$. Finally:

$$\frac{\partial T(\vec{x}, t)}{\partial t} = \alpha\ (\overline{T}^\delta(\vec{x}, t) - T(\vec{x}, t)) \tag{32}$$

with

$$\alpha = \frac{2\Sigma_\delta}{\Omega_\delta} \frac{\lambda}{\rho_s C p_s \delta} = \frac{6\lambda}{\rho_s C p_s \delta^2} \tag{33}$$

which solution reads

$$T(\vec{x}, t) = T(\vec{x}, 0) \exp(-\alpha t) + \int_0^t \overline{T}^\delta(\vec{x}, t')\ \alpha \exp\left[\alpha(t' - t)\right] dt' \tag{34}$$

The gesture that allow to transform (through simple algebra) this equation into one appropriate for Monte Carlo integration consists in rewriting this solution as a unique integral

$$T(\vec{x}, t) = \int_0^\infty \left\{ H(u > t)\ T(\vec{x}, 0) + H(u < t)\ \overline{T}^\delta(\vec{x}, t - u) \right\} \alpha \exp(-\alpha u) du \tag{35}$$

where $H()$ is the Heaviside function. This equation is interpreted in a probabilistic way: the temperature at time t and point $\vec{x}$ can be estimated as the expectation of the random variable $W = H(U > t)\ T(\vec{x}, 0) + H(U < t)\ \overline{T}^\delta(\vec{x}, t - U)$ with U a random variable of law $p(u) =$

$\alpha \exp(-\alpha u)$ and retaining the averaged temperature over the δ-sphere if $u < t$ or the initial temperature $T(\vec{x}, 0)$ if $u > t$. Thanks to double randomization, the average temperature over the δ-sphere, $\overline{T}^{\delta}(\vec{x}, t-u)$, is computed by sampling one value uniformly on the sphere, thus generating a new step of the random walk.

As for the WOS methods, it is necessary to adjust the scheme close to the edge: the approximation made on the spatial dimension is built to ensure the strict accuracy of the scheme at steady state for a tri-linear temperature profile. Note also that the 3D δ-sphere algorithm as been implemented in the example shown here while a simpler 1D random walk could have been used here, due to the horizontal symmetry of the model. It is the same algorithm which is implemented in the `stardis` software used to compute the infrared images of Fig. 4 of the paper, and example of such random walk are displayed in the lower images of this figure. The model could have an infinite depth. Here we choose to impose a depth of 8m which is never reached in practice by the conductive walks.

2.4 Supplementary results for the soil model

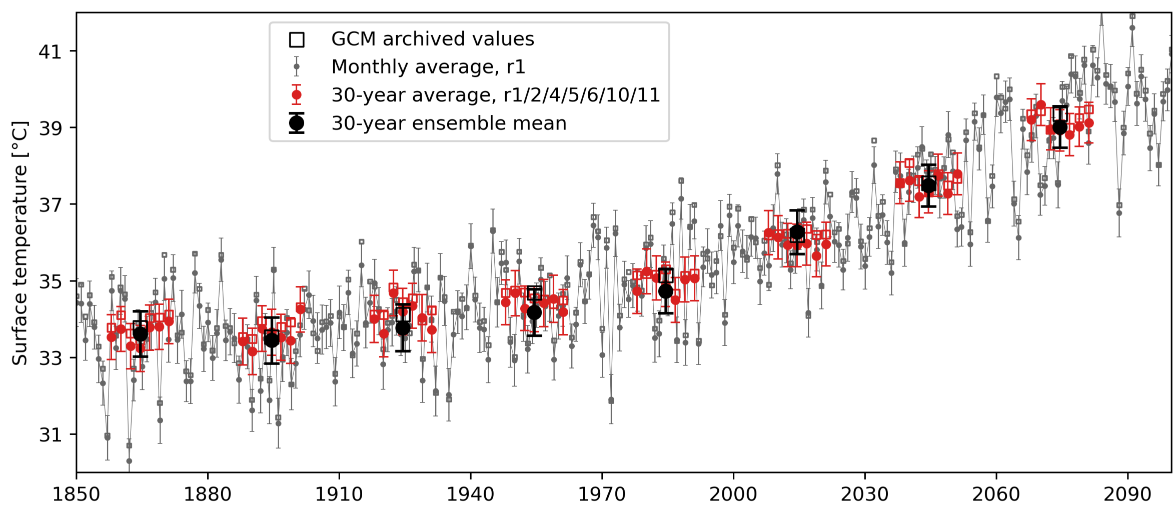

Figure S5. August monthly average of the surface temperature for a point in Sahel. As for Fig. 5e, we show both the year-to-year evolution (gray), the 30-year average (red) and the ensemble 30-year average (black). each dot is computed with 10000 path. The 3-σ error bar is shown as well as the value computed by the climate model, read in the meteorological archive and averaged over the corrseponding period.

Fig. S5 presents a validation of the algorithm for the computation of the surface temperature (see previous sections and schematic in Fig. 5b of the paper). We compare directly the surface temperature of the Monte Carlo simulation with the surface temperature of the climate model, archived in the meteorological datasets. Such a comparison was already presented for a few days in Fig. 5d of the paper ; it is here extended.

Most of the archived temperature felt into the 3-σ error bars. Note however a systematic positive bias of a few tens of K. This biais is not linked to the Monte Carlo approach but to differences in the model between the one integrated on line during the climate simulation, and off line with the Monte Carlo algorithm. The surface temperature in the GCM is computed with a time step of 15 minutes, and the fluxes and atmospheric temperature are made available at a 3 hour frequency only. Because of the non linearity of the coupling (convective in particular), it is not surprising to find differences. At the opposite, the vertical discretization in the soil model is rather coarse in the on line computation. Anyway, the illustration clearly shows the ability of the method to reconstruct surface temperature and its variations, from diurnal to climatic time scales.

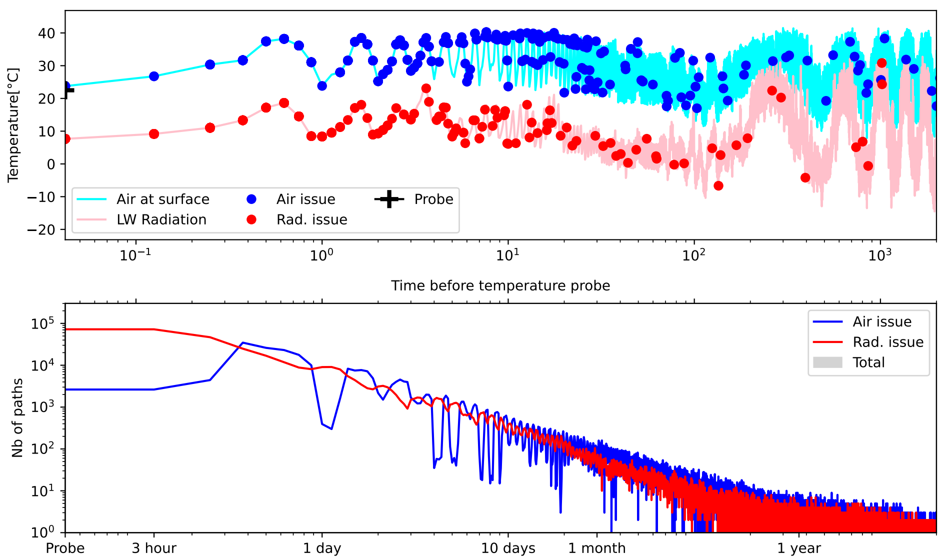

Figure S6. Distribution of the outcomes at T_a or T_{rad} for probe at 04:30:00 on august 1st 2020.

Finally Fig. S6 illustrates the outcomes that contribute to determine the probe temperature (black "+" sign), corresponding of the first day of May 2020 of the meteorological archive. We show both the first 400 values of the outcomes in $\mathbf{T_a}$ and $\mathbf{T_{rad}}$ on the upper graph, with a logarithmic scale in time counted backward from the probe time. The lower graph shows the distribution of the outcomes reconstructed with 10,000,000 paths (leading to a 1-σ uncertainty of less than 0.003 K).

These graphs show how the paths integrate the past history of the atmosphere. The diurnal and seasonal cycle are clearly visible in the upper graph. As stated in the manuscript, the convective coupling of the surface with the atmosphere is much smaller during nighttime than during daytime. As a result, the lower graph shows more radiative outcomes (in red) than convective outcomes (in blue) during nights, whereas the reverse is true during daytime. Altogether, the outcomes (both convective and radiative) in the atmosphere are less frequent at night - the total outcome distribution plotted in grey in the lower graph is lower during nighttime than during daytime - and paths have thus a larger probability to enter the soil for a new conduction random walk.

2.5 Extension to the air conditionning of a room

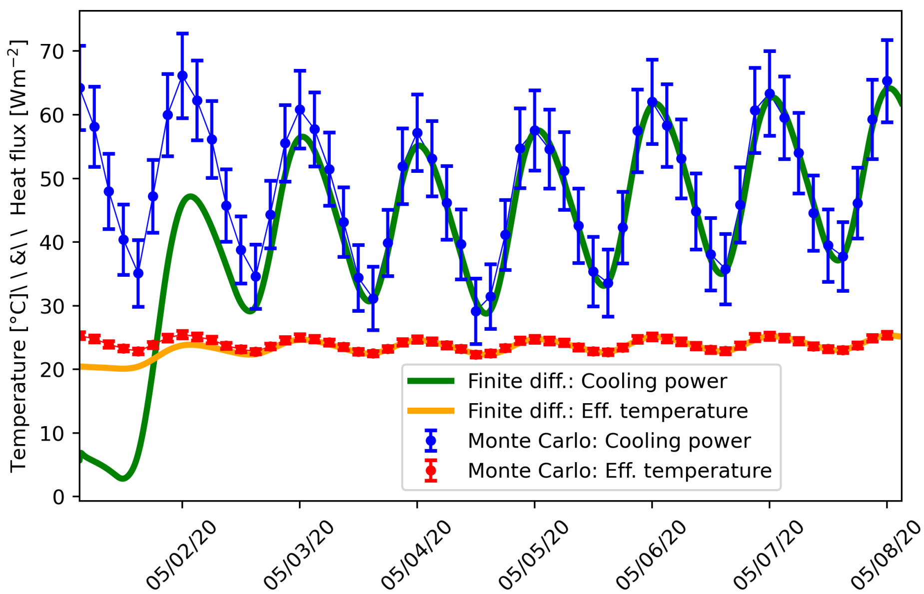

Figure S7. Comparison of the cooling power per unit surface needed to maintain the floor temperature at 293 K. Both the Monte Carlo integration is shown and a finite difference computation, for both the power and a proxy of the associated comfort temperature.

As explained in the manuscript, the computation of the air conditioning is done for the configuration presented in Fig. 5c of the paper and further described in the body of the text. The model for the roof is the same as for the soil in previous sections, except that latent heat fluxes are neglected and that bottom boundary conditions now describe the coupling with a perfectly-mixed room's air model. The roof is a 20 cm slab with density 2400 kg m^{-3}, heat capacity $Cp = 2500$ J kg^{-1} K^{-1} and conductivity 1.5 W m^{-1} K^{-1}, characteristics typical of concrete. The temperature T_{room} of the air of the "room" is coupled by convection to that of the ceiling (the bottom of the roof model), T_{ceil}, and to the imposed temperature of the floor, $T_{floor} =$

293 K, with a coefficient $h_{room,cv}$ =5 W m^{-2} K^{-1}. The ceiling is also coupled radiatively to the floor, with a transfer coefficient $h_{room,rad} = 4\sigma {T_{floor}}^3$. The coupling of the various physics is done with the same approach as in Section 2.2. The power of the air conditioning needed to maintain the floor's temperature at its setpoint value T_{floor} is computed as

$$P = h_{room,rad}(T_{ceil} - T_{floor}) + h_{room,cv}(T_{room} - T_{floor}) \tag{36}$$

This sum itself is treated in a probabilistic way, together with the other dimensions of the problem. Note that the formula is valid here because the two terms do not change sign in the hot Sahelian condition considered here. The very simple model used here allows an easy derivation of an equivalent 1D finite difference code. Fig. S7 presents the comparison of such an estimation with the Monte Carlo computation for a few days in May 2020. The power needed for cooling per unit surface is shown as well as a proxy of the comfort temperature computed as the

$$T_{eff} = T_{floor} + \frac{P}{h_{room,rad} + h_{room,cv}} = \frac{h_{room,rad}T_{ceil} + h_{room,cv}T_{room}}{h_{room,rad} + h_{room,cv}} \tag{37}$$